

Thin Film Processing of Photorefractive BaTiO₃

NASA Research Grant NAG-1-1247

First semi-annual progress report to

Dr. Sharon Welch
NASA Langley Research Center
Hampton, Virginia 23665

(NASA-CR-192194) THIN FILM
PROCESSING OF PHOTOREFRACTIVE
BaTiO₃ Semiannual Progress Report
No. 1 (JHU) 22 p

Principal Investigator:

Dr. Paul R. Schuster
(301) 953-6239

Co-Principal Investigator

Dr. Richard S. Potember
(301) 953-6251

ORIGINAL CONTAINS
COLOR ILLUSTRATIONS

October 1991

Advanced Materials Program
Applied Physics Laboratory
The Johns Hopkins University
Laurel, MD 20723-6099

TABLE OF CONTENTS

| | |
|---------------------------------|----|
| I. Objectives..... | 1 |
| II. Materials Preparation..... | 1 |
| Sol-gel..... | 1 |
| Sputtering..... | 3 |
| Pulsed-laser Ablation..... | 3 |
| III. Analytical Techniques..... | 5 |
| IV. Future Work..... | 7 |
| Materials Preparation..... | 7 |
| Poling..... | 9 |
| Analytical Techniques..... | 10 |
| Optical Characterization..... | 11 |
| V. References..... | 11 |
| Figures..... | 13 |

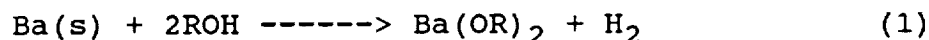
I. OBJECTIVES:

The principle objectives of this ongoing research involve the preparation and characterization of polycrystalline single-domain thin films of BaTiO_3 for photorefractive applications. These films must be continuous, free of cracks, and of high optical quality. The two methods proposed are sputtering and sol-gel related processing.

II. MATERIALS PREPARATION:

SOL-GEL:

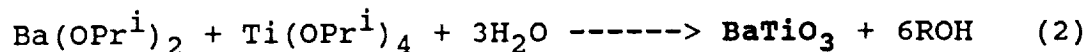
In our development of the sol-gel technique for synthesis of BaTiO_3 , we have begun with the alkoxides of both barium and titanium. Titanium isopropoxide, $\text{Ti}(\text{OPr}^i)_4$, is commercially available, still redistillation is usually required in order to obtain the desired purity. Barium isopropoxide, $\text{Ba}(\text{OPr}^i)_2$, is much more difficult and costly to obtain due to its unstable nature. We have prepared our own barium isopropoxide by dissolving barium metal (anhydrous) in isopropanol.



where R is an alkyl radical.

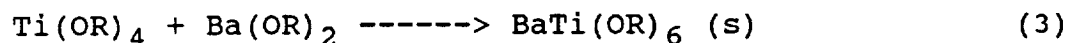
The concentrations of the two metal alkoxides must be adjusted to equimolar in order to obtain the correct stoichiometry (barium:titanium - 1:1) in our final product.

The desired net reaction is the simultaneous hydrolytic decomposition of titanium and barium isopropoxide.



There are a number of intermediate reactions that take place resulting from the difference in the rates of hydrolysis of the two metal alkoxides. This poses a problem because the titanium is almost completely hydrolyzed before the barium has enough time to react. Also precipitates form almost immediately which eliminated the possibility of film preparation from this solution. The low yield that we obtained in the powder form was calcined at various temperatures ranging from 500 to 1000°C, but all samples exhibited on X-ray diffraction only slight traces of crystallinity.

An alternative method of processing is concurrently being investigated. A direct anhydrous mixture of the isopropoxide solutions eliminates the preliminary hydrolysis reaction and thereby also eliminates the undesirable hydroxide precipitate.



The precipitate that forms from this reaction serves as a precursor for subsequent hydrolysis and condensation reactions in the thin film preparation. However, an

intermediate product of crystalline BaTiO_3 powder can be formed by direct heat treatment of the BaTi(OR)_6 solid.

When the heat treatment of BaTi(OR)_6 does produce a polycrystalline BaTiO_3 powder, it is then reasonable to assume this solution will also yield a polycrystalline BaTiO_3 film. The remaining BaTi(OR)_6 compound must be redissolved in an appropriate solvent. A more in-depth evaluation of the available solvents needs to be performed, but it appears that hexyl alcohol and toluene are two possibilities. A minimal amount of solvent is desirable, so as to increase the viscosity of the solution for both dip and spin coating.

The substrates chosen for these initial studies were both n-type (100) and p-type (111) single crystal silicon wafers. Other sol-gel derived ferroelectric films have been successfully deposited on silicon even though there exists a lattice mismatch and a difference in thermal expansion coefficients [1]. The silicon substrate allows for the measurement of certain electrical properties of particular interest, such as ferroelectricity. A ferroelectric response is critical for photorefractive barium titanate.

SPUTTERING:

Pulsed-laser Ablation:

The pulsed-laser ablation technique has recently shown potential as another method for ferroelectric thin film deposition [2,3]. This technique is similar to rf and dc

sputtering, but utilizes high energy radiation from a laser instead of an ionized gas (plasma) from an electric discharge.

Initial laser ablation studies have already taken place. The first sample has yet to be fully characterized, but was deposited on a 1 mm thick single crystal of barium titanate. This substrate was provided to us by Dr. Daniel Rytz at Sandoz Corporation. The face on which deposition took place was polished to better than $\lambda/8$. The target material was a slice from a single crystal boule of BaTiO_3 and was neither polished nor poled.

Film deposition was accomplished through the use of an excimer laser ($\lambda=193$ nm) operating at an energy level of 75 mJ/pulse and a repetition rate of 10 Hz. The laser beam spot size at the target was $6 \times 10^{-2} \text{ cm}^2$, and the target was 3.5 cm from the substrate. The substrate was maintained at a temperature of 750°C under 420 mTorr of oxygen atmosphere. In an attempt to deposit a film greater than a micron thick, the target was exposed to 12,000 pulses of radiation. The laser was rastered over the target in order to avoid preferential wear. After deposition, cooling of the film was performed at a slow rate under atmospheric pressure of oxygen. An initial drop in temperature from 750°C to 650°C occurred within three minutes, but the film was then held at 650°C for 27 minutes and finally brought down to room temperature at a rate of 5°C/minute.

III. ANALYTICAL TECHNIQUES:

Optical microscopy is used for initial sol-gel film evaluation both before and after the heat treatment (Figs. 1,2). The condition of the film including its thickness and uniformity can be qualitatively assessed. Surface profilometry generates quantitative information concerning the film thickness and the surface roughness. Results indicate that the current synthetic procedure produces a relatively smooth film that is about 1,000 Å thick per coat applied.

Thermogravimetric analysis is useful in determining the heat treatment parameters. As stated by Mosset et al. [4], there are three temperature regions within the heat treatment process. From 0 to 250°C solvents are driven off. At temperatures ranging from 250 to 400°C solvents continue to be driven off and decomposition of the organics is initiated. From 400 to 650°C the solid phase begins to go through a transformation from an amorphous state to a crystalline state (Fig. 3).

Once the heat treatment has been performed the degree of crystallinity can be assessed by X-ray diffraction. Also the crystal structure with some indication of stoichiometry can be determined. It is useful to analyze the BaTiO₃ powder, which is formed as an intermediate product, by X-ray diffraction before casting a film. This gives further insight into the heat treatment parameters required for crystalline film formation. Our powder diffraction results

do show polycrystalline peaks. These peaks correlate reasonably well with data from the Joint Committee on Powder Diffraction Standards [5] for tetragonal BaTiO_3 . However the signal to noise ratio is poor, and the background characteristics (parabolic) seem to indicate the existence of amorphous material (Fig. 4).

Even if crystallinity of our samples is established by X-ray diffraction, the correct crystalline structure (tetragonal phase at room temperature) must be ascertained. Since BaTiO_3 is ferroelectric in the tetragonal phase, a modified Sawyer-Tower circuit [6] has been built to examine the ferroelectric behavior of our samples (Fig. 5). The results obtained on a number of our samples are in agreement with the data acquired through X-ray diffraction. The deformed hysteresis loop (Fig. 6) is indicative of incomplete crystallization, as was revealed by the diffraction pattern discussed earlier.

Other methods for characterizing both the condition of the film and the stoichiometry include scanning electron microscopy (SEM) with X-ray compositional analysis. SEM photomicrographs show stress induced cracking in a number of the films and a precipitate is also discernable (Figs. 7,8). Results from the X-ray diffraction studies, the ferroelectric response, and the SEM photomicrographs give a strong indication that the heat treatment must be dramatically altered. A higher temperature must be attained

for complete crystallization to take place, and the cooling rate must be reduced to minimize thermal stress.

X-ray compositional analysis identifies certain elements which are present within the films and can be useful as a semi-quantitative tool for stoichiometric evaluation. In order to maximize the quantitative information obtained through this technique, a small BaTiO_3 sample from a bulk single crystal was analyzed as a reference for comparison. The characteristics of interest include the ratios of the titanium $K\alpha$ and the barium $L\alpha$ peaks, and the percentage of the titanium versus the barium oxide. Initial data show a fairly good correlation with the reference, indicating that the stoichiometry of our samples is close to that desired (Figs. 9,10).

Atomic force microscopy is a powerful analytical tool for the study of surface morphology. The resolution attained with this technique yields detailed information concerning the surface features of our films. Photomicrographs of one sample reveal a smooth surface with grain size approximating 500 Å (Figs. 11,12).

IV. FUTURE WORK:

MATERIALS PREPARATION:

In order to make the sol-gel technique more applicable for thin film deposition of BaTiO_3 , the rates of hydrolysis of the two metal alkoxides must be altered. One possible

approach is the addition of 2-ethylhexanoic acid (2EHA) to the alkoxide solution. This approach has been successfully used to stabilize and inhibit precipitation in the formation of both sol-gel derived PZT films [7] and films of superconducting $\text{YBa}_2\text{Cu}_3\text{O}_{7-x}$ [8]. We will have to stabilize the alkoxide solution at various concentrations in order to evaluate the different methods for film application. Viscosity is a key parameter in film application techniques such as spin coating, dip coating, and spray coating.

A related technique called metallo-organic decomposition has recently been successful in the deposition of a wide variety of thin film materials and is therefore also of interest [9]. This technique differs from sol-gel processing in that a gel is never formed, and the compound requirements are considerably different. One major advantage is that the precipitate that forms as a result of the sol-gel process, will not form once the metallo-organic is put into solution. Metallo-organics, such as those formed by combining a metal ion with a carboxylic acid, have been found to have high solubility in many solvents and wet most substrates [9]. Possible precursors for the formation of thin film BaTiO_3 are barium neodecanoate $[\text{Ba}(\text{C}_9\text{H}_{19}\text{COO})_2]$ and titanium dimethoxy dineodecanoate $[(\text{CH}_3\text{O})_2\text{Ti}(\text{C}_9\text{H}_{19}\text{COO})_2]$ [10]. For the formation of the film, it will also be necessary to study various concentrations of the metallo-organic solution.

Sputtering of BaTiO_3 will be performed along with related techniques such as pulsed-laser ablation. We have prepared both target and substrate materials. A number of parameters still need to be fully evaluated in order to produce optimum films. These parameters include the oxygen pressure, incident energy, beam spot size, substrate temperature, cooling rate, and distance between substrate and target.

Substrates will include transparent (in the visible) materials, such as fused silica, for optical applications. Other ferroelectrics, such as $\text{Sr}_x\text{Ba}_{1-x}\text{Nb}_2\text{O}_6$, have been successfully deposited on fused silica substrates [1]. Substrate parameters to be considered include orientation, thermal expansion coefficients, and heat treatment during and after deposition.

POLING:

Poling will be attempted both during the actual deposition of the films and after deposition has taken place. Electrical poling will be attempted by applying a constant electric field during cooling from the paraelectric phase (nonpolar) through the Curie temperature into the ferroelectric phase. Since the paraelectric phase (cubic) is higher in symmetry than the ferroelectric phase (tetragonal), there is a possibility for crystallographic twinning [11]. These twins can be prevented or removed by application of a uniaxial stress as part of the poling

process. Switching reverse domains is also possible below the Curie temperature by application of a constant electric field which is greater than the coercive field. With either poling approach, the electric field must be held constant within the crystal at a level approximating 2-5 kV/cm [12,13]. This can only be accomplished when the electrodes and the polar faces are in direct contact. In this way depolarization fields do not present a problem.

ANALYTICAL TECHNIQUES:

Other analytical techniques such as Fourier transform - infrared spectroscopy are being considered for analysis of the precursors and the final product. The infrared spectrum gives important information on the molecular structure of the various compounds through vibrations between the atoms within each molecule.

The success of the poling procedure must also be determined. Since the optical frequency susceptibility is anisotropic in tetragonal BaTiO_3 , domain observation both before and after poling may be performed by viewing the crystals between crossed polarizers (providing that the polar axis of the crystal and the polarizer axes are not coplanar) [14]. Other techniques for poling evaluation include chemical etchants which etch the positive and negative ends of domains at different rates (HCL and HF for BaTiO_3) [15], and the pyroelectric technique which involves the change in the spontaneous polarization with the sample

due to thermal energy on heating [16]. This change in spontaneous polarization produces free charges at the crystal surface, whose sign is dependent on the charge distribution within the domains.

OPTICAL CHARACTERIZATION:

Single crystal samples of bulk BaTiO_3 have been used in the analytical process in an attempt to establish a standard for comparison. Also optical measurements were made on a poled single crystal of barium titanate to generate reference data. Optical measurements which are being performed include energy transfer within two beam coupling, dynamic holography (diffraction efficiency), response time, four wave mixing for phase conjugate reconstruction, optical storage, and self-pumped phase conjugation. Once we have determined that our films have the correct structure and stoichiometry, optical measurements will be conducted on the films, and a direct comparison will be made with the data acquired from the single crystal BaTiO_3 sample.

V. REFERENCES:

- 1) C.J. Chen, Y. Xu, R. Xu, and J.D. Mackenzie, J. Appl. Phys. **69** (3), 1763 (1991).
- 2) R. Nawathey, R. Vispute, S.M. Chaudhari, S.M. Kanetkar, and S.B. Ogale, Solid State Commun. **71** (1), 9 (1989).
- 3) M.G. Norton, G.R. English, and C.B. Carter, Mat. Res. Soc. Symp. Proc. **200**, 237 (1990).

- 4) A. Mosset, I. Gautier-Luneau, J. Galy, P. Strehlow, and H. Schmidt, *J. Non-Cryst. Solids* **100**, 339 (1988).
- 5) Powder Diffraction File - Inorganic Sets 1-5, edited by L.G. Berry (Joint Committee on Powder Diffraction Standards, Philadelphia, 1974) p. 654.
- 6) C.B. Sawyer and C.H. Tower, *Phys. Rev.* **35**, 269 (1930).
- 7) K.C. Chen, "Ferroelectric Lead Zirconate Titanate Films from Metallo-organic Precursors," Ph.D. Dissertation, Univ. of California, Los Angeles (1989).
- 8) H. Zheng and J.D. Mackenzie, Unpublished results.
- 9) J.V. Mantese, A.L. Micheli, A.H. Hamdi, and R.W. Vest, *Materials Research Society Bulletin*, 48 (1989).
- 10) J.J. Xu, A.S. Shaikh, and R.W. Vest, *IEEE Trans. Ultrason. Ferroelec. Freq. Contr.* **36** (3), 307 (1989).
- 11) M.E. Lines and A.M. Glass, Principles and Applications of Ferroelectrics and Related Materials (Clarendon Press, Oxford, 1979) pp. 127-128.
- 12) M.B. Klein and G.C. Valley, *J. Appl. Phys.* **57** (11), 4901 (1985).
- 13) M.B. Klein and R.N. Schwartz, *J. Opt. Soc. Am. B* **3** (2), 293 (1986).
- 14) F. Jona and G. Shirane, Ferroelectric Crystals (Pergamon Press, New York, 1962) pp 160-161.
- 15) G. Arlt & P. Sasko, *J. Appl. Phys.* **51** (9), 4956 (1980).
- 16) M.E. Lines and A.M. Glass, Principles and Applications of Ferroelectrics and Related Materials (Clarendon Press, Oxford, 1979) p. 92.

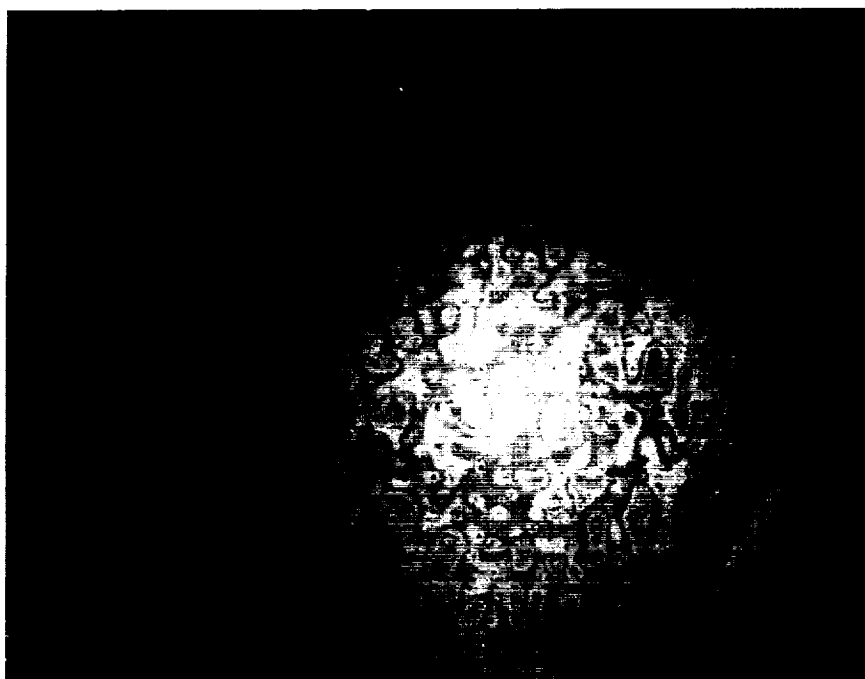


Figure 1. Representative sample before heat treatment.

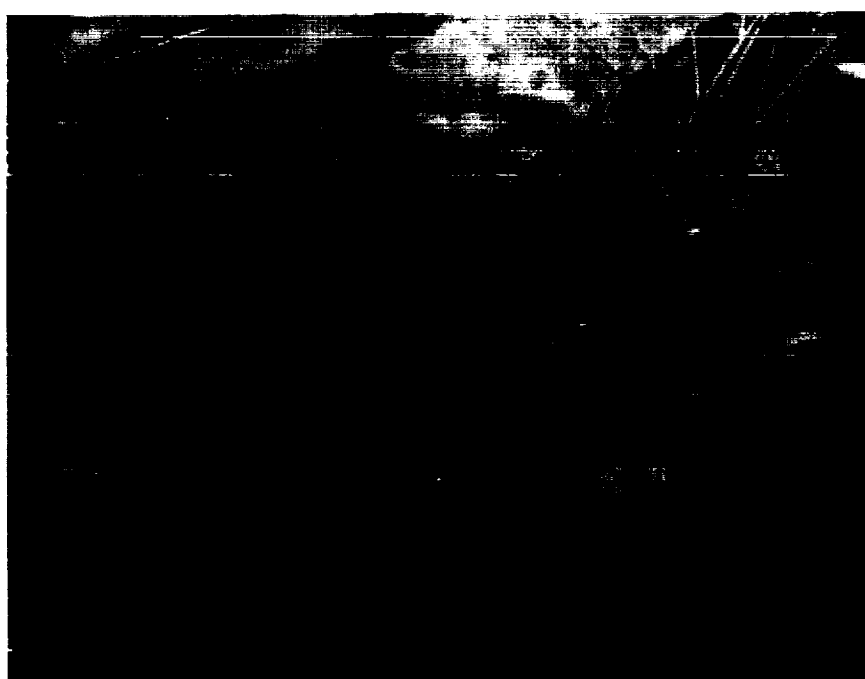


Figure 2. Representative sample after heat treatment.

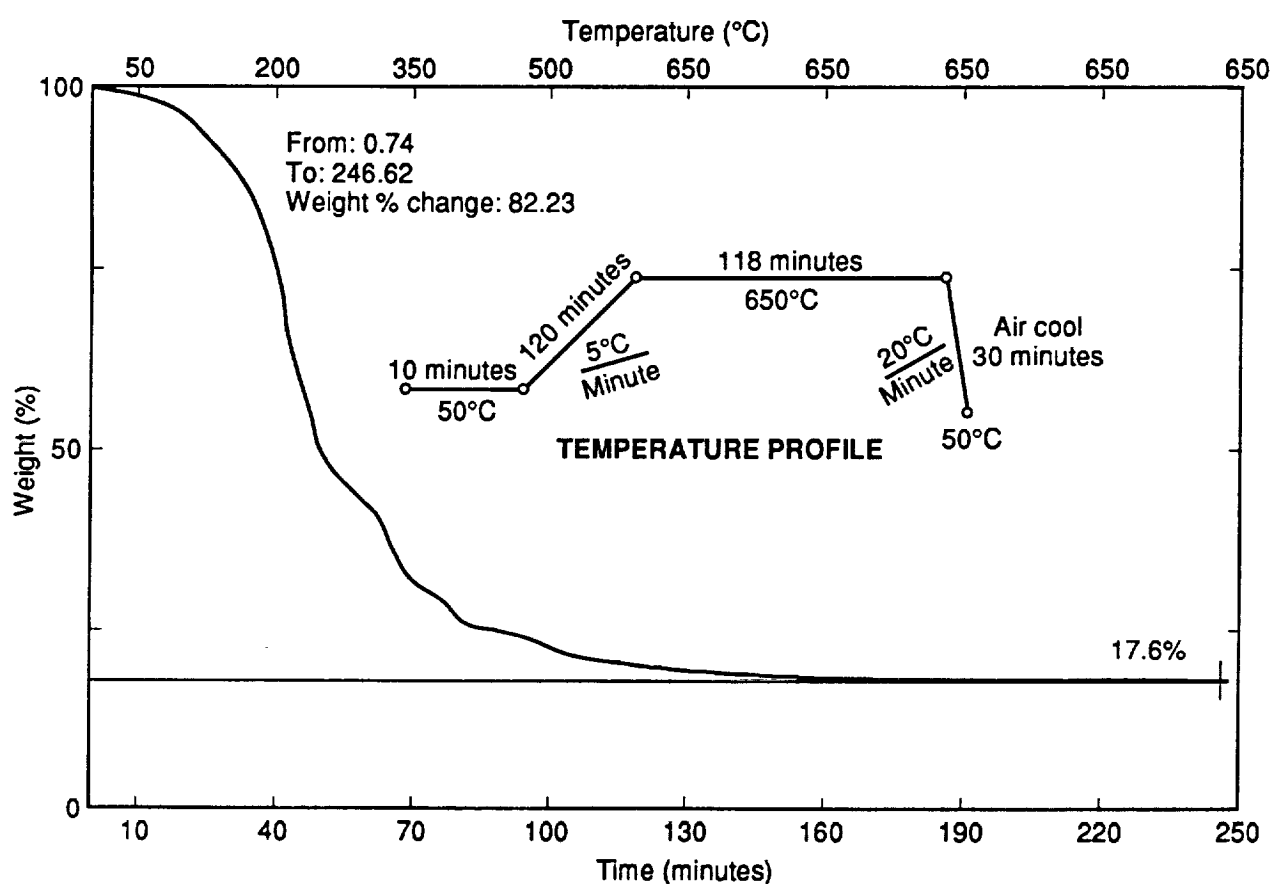


Figure 3. Thermogravimetric analysis indicates that the majority of the weight loss occurs prior to attaining the maximum temperature of 650°C. However, residual weight loss continues even at 650°C. The temperature profile identifies the heat treatment process used in this experiment.

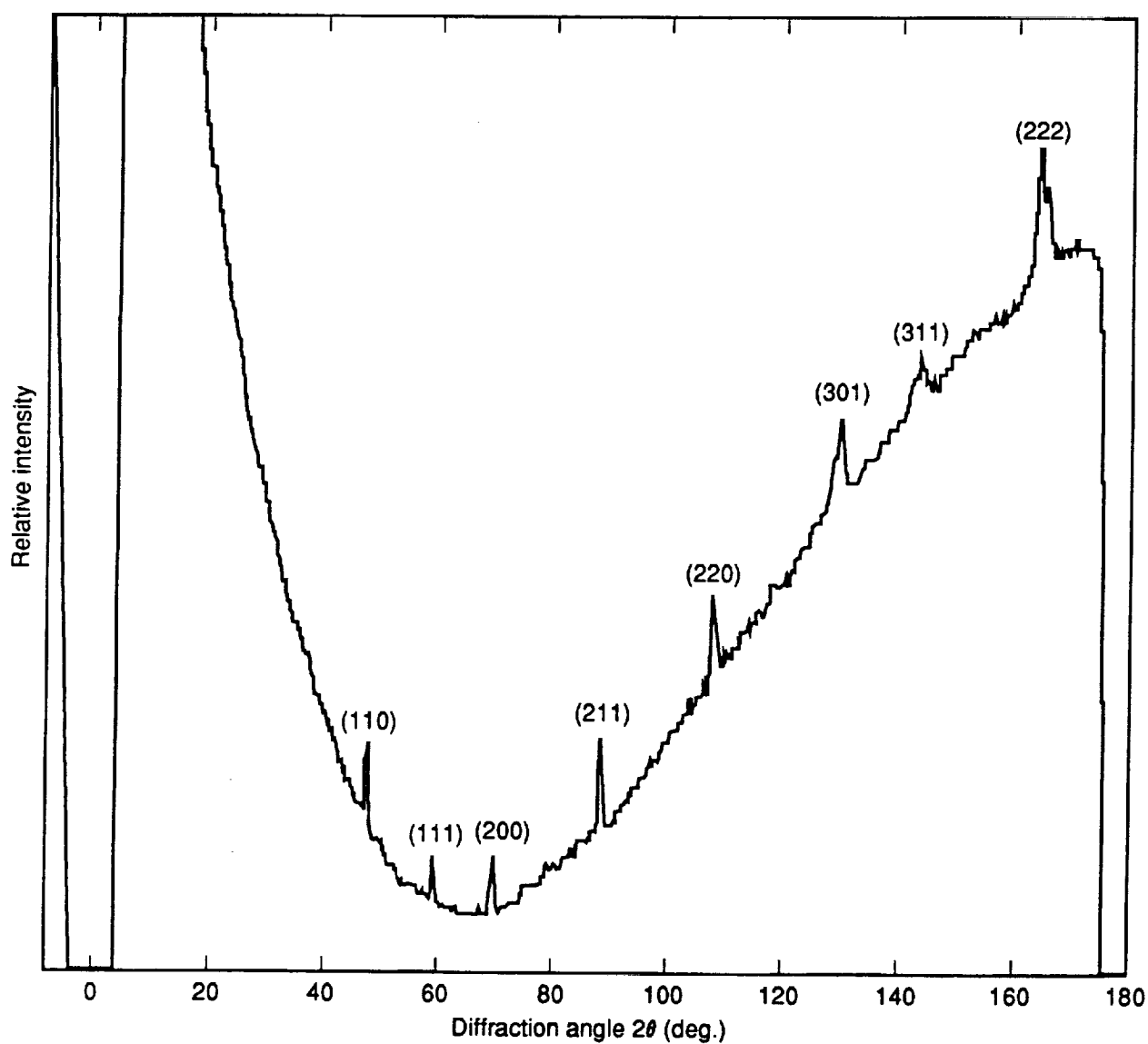


Figure 4. Powder X-ray diffraction pattern exhibits both tetragonal crystallinity (peaks) and amorphous material (parabolic background). The diffraction planes are indicated by their Miller (hkl) indices. Radiation source was the chromium $K\alpha$ line ($\lambda=2.29092$).

V_1 is $\approx 0 - 20V$ at 60 Hz

$R_1 = R_2 = 0.1 \text{ M } \Omega$

R_3 is variable $\approx 1 \text{ k } \Omega$ to $1 \text{ M } \Omega$

C_1 is variable $\approx 0.001 \mu\text{f}$ to $1.0 \mu\text{f}$

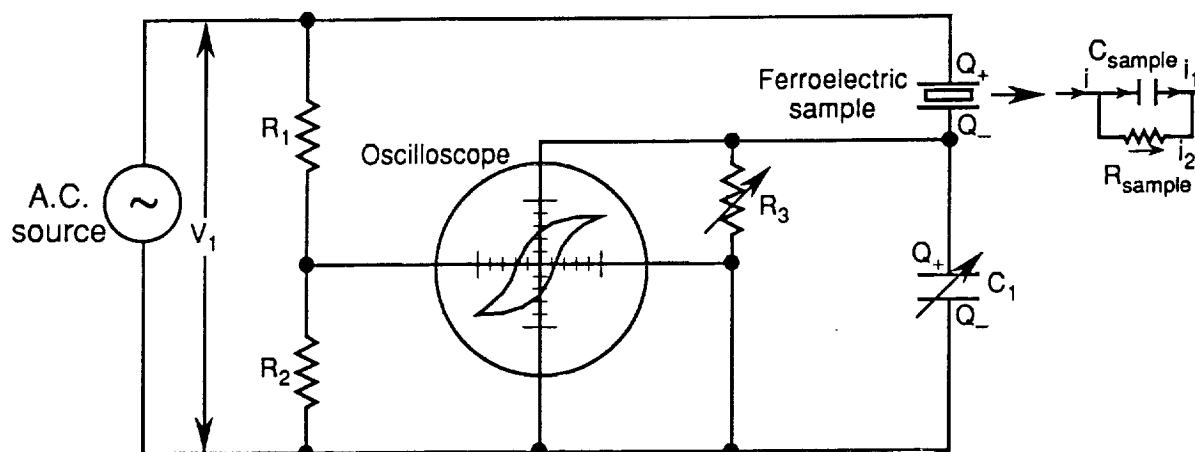


Figure 5. Modified Sawyer-Tower circuit for ferroelectric analysis.

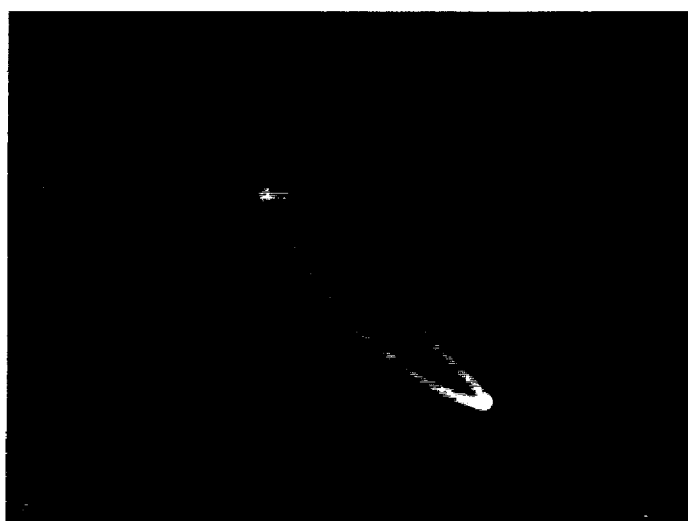


Figure 6. Distorted hysteresis loop indicative of incomplete crystallization and induced thermal stress within the film.



Figure 7. SEM photomicrograph showing thermal stress induced cracking.



Figure 8. SEM photomicrograph showing both thermal stress induced cracking and precipitate formation.

ORIGINAL PAGE
COLOR PHOTOGRAPH

BAT103REF2

| | |
|-------------------------------|--------------|
| Accelerating voltage | 20.0 KeV |
| Beam - sample incidence angle | 45.0 degrees |
| Xray emergence angle | 22.1 degrees |
| Xray - window incidence angle | 90.0 degrees |
| Window thickness | 20.0 microns |

STANDARDLESS EDS ANALYSIS
(ZAF CORRECTIONS VIA MASC V)

| ELEMENT & LINE | K-RATIO** | WEIGHT PERCENT | PRECISION 2 SIGMA | OXIDE FORMULA | OXIDE PERCENT | NO. OF CATIONS IN FORMULA |
|-------------------|-----------|-------------------|----------------------|------------------|------------------|------------------------------|
| Al KA | 0.0000 | 0.00 | 0.00 | Al2O3 | 0.00 | 0.0000 |
| Si KA | 0.0000 | 0.00 | 0.00 | SiO2 | 0.00 | 0.0000 |
| Ti KA | 3.6439 | 43.53 | 0.17 | TiO2 | 72.61 | 1.3638 |
| Fe KA | 0.0000 | 0.00 | 0.00 | FeO | 0.00 | 0.0000 |
| Co KA | 0.0000 | 0.00 | 0.00 | CoO | 0.00 | 0.0000 |
| Ba LA | 0.3541 | 24.54 | 0.11 | BaO | 27.39 | 0.2685 |
| Au LA | 0.0000 | 0.00 | 0.00 | Au | 0.00 | 0.0000 |
| O O | | 31.94 | | | | |
| TOTAL | | | | | 100.01 | 1.6342 |

* DETERMINED BY STOICHIOMETRY
NUMBER OF CATIONS CALCULATED ON BASIS OF 3 OXYGEN ATOMS.

**NOTE: K-RATIO = K-RATIO * R
where R = reference(standard)/reference(sample)

NORMALIZATION FACTOR: 1.268

GAUSSIAN DECONVOLUTION
SAMPLE: BAT103REF2

WINDOW 1 : 3.77 - 6.00 kev

0 sec. acquisition time

| Lines of Interest | Intensity (cts/sec) | 2-sigma error (relative) | Standard spectrum | K-ratio |
|-------------------|---------------------|--------------------------|-------------------|---------|
| Al KA | 0.00 | 0.0000 | | |
| Si KA | 0.00 | 0.0000 | | |
| Ti KA | 466.44 | 0.0038 | | |
| Fe KA | 0.00 | 0.0000 | | |
| Co KA | 0.00 | 0.0000 | | |
| Ba LA | 255.69 | 0.0044 | | |
| Au LA | 0.00 | 0.0000 | | |

CHI-SQUARED: 3.9326

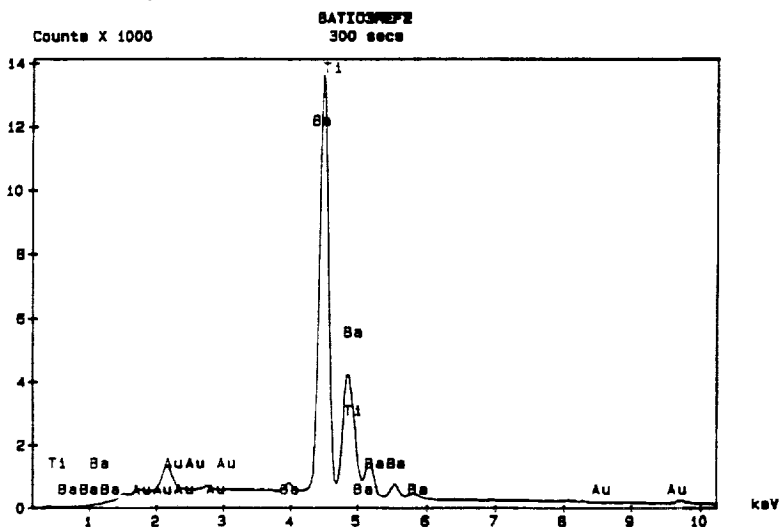


Figure 9. The results from X-ray compositional analyses of BaTiO₃ single crystals provide reference data for comparative studies with our samples. The ratios of both the oxide percentages (TiO₂ to BaO) and the intensities of the titanium K α peak to the barium L α peak are equal to 2.65:1 and 1.82:1 respectively.

BAT103_FILM2A

Accelerating voltage 20.0 KeV
 Beam - sample incidence angle 45.0 degrees
 Xray emergence angle 22.1 degrees
 Xray - window incidence angle 90.0 degrees
 Window thickness 20.0 microns

STANDARDLESS EDS ANALYSIS
(ZAF CORRECTIONS VIA MAGIC V)

| ELEMENT & LINE | K-RATIO** | WEIGHT PERCENT | PRECISION 2 SIGMA | OXIDE FORMULA | OXIDE PERCENT | NO. OF CATIONS IN FORMULA |
|-------------------|-----------|-------------------|----------------------|------------------|------------------|------------------------------|
| Ti KA | 0.6296 | 22.67 | 0.18 | TiO2 | 71.18 | 1.3559 |
| Ba LA | 0.3704 | 25.81 | 0.12 | BaO | 28.82 | 0.2863 |
| O O | | 31.51 | | | | |
| TOTAL | | | | | 99.99 | 1.6421 |

* DETERMINED BY STOICHIOMETRY

NUMBER OF CATIONS CALCULATED ON BASIS OF 3 OXYGEN ATOMS.

**NOTE: K-RATIO = K-RATIO * R
where R = reference(standard)/reference(sample)

NORMALIZATION FACTOR: 1.125

GAUSSIAN DECONVOLUTION

SAMPLE: BAT103_FILM2A

WINDOW 1 : 3.65 - 6.13 kev

0 sec. acquisition time

| Lines of Interest | Intensity (cts/sec) | 2-sigma error (relative) | Standard spectrum | K-ratio |
|-------------------|---------------------|--------------------------|-------------------|---------|
| Ti KA | 374.54 | 0.0043 | | |
| Ba LA | 220.36 | 0.0047 | | |

CHI-SQUARED: 2.1845

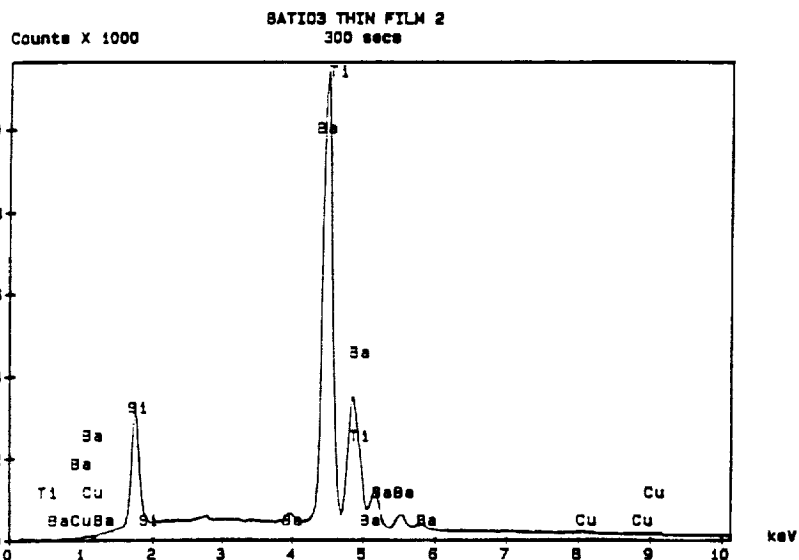


Figure 10. X-ray compositional analyses performed on BaTiO₃ films demonstrate the existence of the key elements at proportions which are similar to those of the reference. The ratios of both the oxide percentages (TiO₂ to BaO) and the intensities of the titanium K α peak to the barium L α peak are equal to 2.47:1 and 1.7:1 respectively.

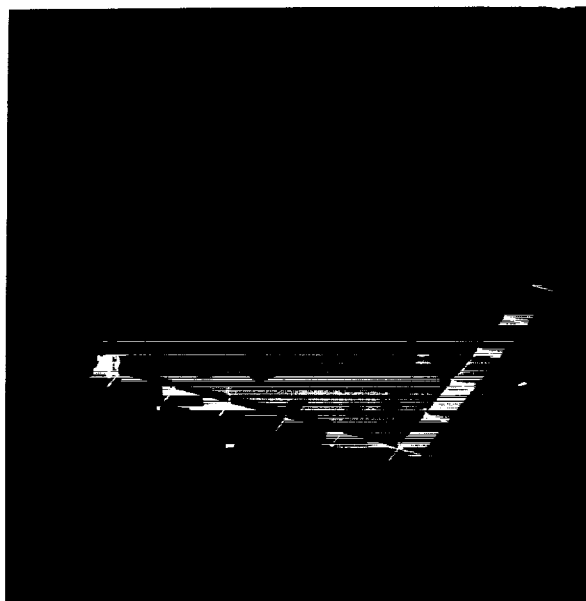


Figure 11. Photomicrograph from the atomic force microscope reveals a smooth but somewhat porous film.

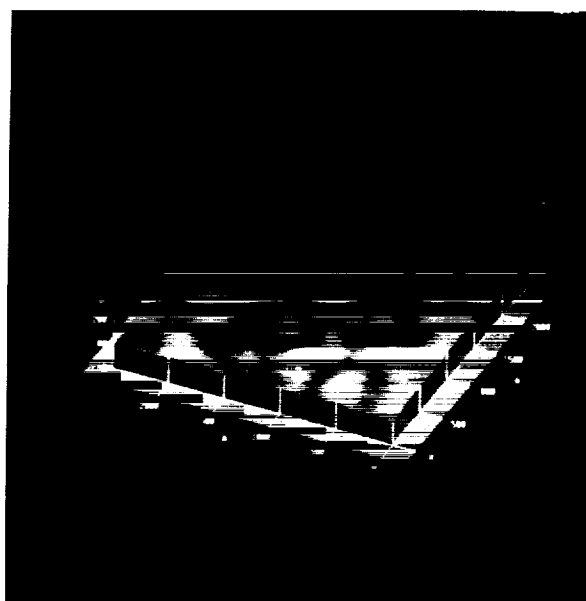


Figure 12. At higher magnification the atomic force microscope reveals the approximate grain size (500 Å) of the film.